Published in final edited form as:
Proc IEEE Conf Decis Control. 2013 ; : 121–126. doi:10.1109/CDC.2013.6759869.

A Predictive Model for the Anticoagulant Bivalirudin Administered to Cardiac Surgical Patients*

Qi Zhao[†], **Thomas Edrich**[‡], and **Ioannis Ch. Paschalidis**[§]

[†]Division of Systems Engineering, Boston University, Boston, MA 02215, zhaoqi@bu.edu

[‡]Department of Anesthesia, Perioperative and Pain medicine, Brigham and Women's Hospital, Boston, MA 02215, tedrich@partners.org

[§]Dept. of Electrical & Computer Eng., Division of Systems Eng., and Center for Information & Systems Eng., Boston University, 8 St. Mary's St., Boston, MA 02215, yannisp@bu.edu, url: http://ionia.bu.edu/

Abstract

Bivalirudin is used in patients with heparin-induced thrombocytopenia and is a direct thrombin inhibitor. Since it is a rarely used drug, clinical experience with its dosing is sparse. We develop a model that predicts the effect of bivalirudin, measured by the *Partial Thromboplastin Time (PTT)*, based on its past fusion rates. We learn population-wide model parameters by solving a nonlinear optimization problem that uses a training set of patient data. More interestingly, we devise an adaptive algorithm based on the extended Kalman filter that can adapt model parameters to individual patients. The latter adaptive model emerges as the most promising as it reduces both the mean error and, drastically, the per-patient error variance. The model accuracy we demonstrate on actual patient measurements is sufficient to be useful in guiding optimal therapy.

I. Introduction

Bivalirudin is infused as a "blood thinner" in patients who have or are suspected of having blood clots or risk of blood clotting and who have a contraindication to heparin. It is infused continuously, and is eliminated via the kidneys and by plasma protease-metabolism [2], [6], [7]. It affects the blood coagulation parameters *Partial Thromboplastin Time (PTT)* and the *International Normalized Ratio (INR)* in a dose-dependent fashion. Both measure the ability of the blood to clot but while PTT is measured in seconds, INR is a dimensionless number.

As a rarely used drug, bivalirudin is used more frequently in the cardiac *Intensive Care Unit (ICU)* but residents adjusting the infusion rate have little experience, resulting in overdosing or underdosing. Adequate anticoagulation is necessary to avoid the risk of clot formation, but overshooting increases the risk of bleeding. There is considerable inter-and intra-

*Research partially supported by the NIH/NIGMS under grant GM093147, by the NSF under grants CNS-1239021 and IIS-1237022, by the ARO under grants W911NF-11-1-0227 and W911NF-12-1-0390, by the ONR under grant N00014-10-1-0952, and by the STAR (Surgical ICU TrAnslational Research) Center at Brigham and Women's Hospital. T. Edrich and I. Ch. Paschalidis are equal contributors to the research.

Correspondence to: Ioannis Ch. Paschalidis.

individual variability in the response to bivalirudin. For this reason, a mathematical model that predicts the PTT based on the past infusion rates of bivalirudin following dose adjustment would be useful to guide optimal therapy.

In earlier work [4], [3], we have built a simple one-state linear system model to describe the effect of bivalirudin in patients. The models were designed using Matlab/simulink (Mathworks, Natick, MA) and default parameter identification procedures. Motivated by this work, in the present paper we develop a method to predict PTT values based not only on past bivalirudin infusion rates but also on a host of patient-specific physiological variables that characterize blood composition, renal, and liver function. The results we obtain substantially improve accuracy compared to our earlier work.

More specifically, we develop a more complex dynamic system model than the one developed in [4], [3]. This new model takes the elimination of bivalirudin by the kidneys and liver into account. We identify model parameters by formulating a nonlinear optimization problem that minimizes the ℓ_2 norm of the prediction error over a training set of measurements. To solve this problem we leverage quasi-Newton methods. Building on this model, we develop an adaptive on-line algorithm based on the extended Kalman filter than can adapt the model parameters to individual patients. The algorithm starts from population-wide optimal parameters and as it observes inputs and outputs it modifies model parameter values to better fit an individual patient. This adaptive model slightly reduces the average prediction error compared to the population-wide model and substantially reduces the per-patient error variability, in fact by a factor of about 2.5, which is significant.

The approach we develop in this work is general and can be applicable to a host of related problems. As ICUs and hospital wards accelerate the digitization of patient records, tremendous opportunities arise for automated and mathematically rigorous patient monitoring and medication dosing. It is in such a framework that the methods we develop can become useful.

The remainder of the paper is organized as follows. Section II presents the dynamic system model. Section III develops the extended Kalman filter to achieve model parameter adaptation. Finally, concluding remarks appear in Section IV.

Notation: We use bold letters to denote vectors and matrices; typically vectors are denoted by lower case letters and matrices by upper case letters. Vectors are assumed to be column vectors unless explicitly stated otherwise. For economy of space we write $\mathbf{x} = (x_1, \ldots, x_n)^T$ for the n-dimensional column vector $\mathbf{x} \in \mathbb{R}^n$. Prime denotes transpose, $\|\cdot\|$ denotes the Euclidean norm, $\mathbf{0}$ denotes a vector or matrix with all components set to zero, and $\mathbf{I}$ is the identity matrix.

II. An dynamic system model

This section introduces a *Multiple Input Single Output (MISO)* dynamic system model that attempts to explicitly account for the way bivalirudin affects PTT values in patients.

A. The predictors

In our problem, we have clinical data from 233 patients. The key quantity (response) we would like to predict is the *Partial Thromboplastin Time (PTT)*, denoted by $y_i(t)$, of each patient i at each time t. As predictors we include 11 key physiological variables sampled over M consecutive time instants $t > t - \tau_1 > \cdots > t - \tau_{M-1}$ where τ_m for $m = 1, \ldots, M - 1$ denote the time lags between consecutive measurements, which are not necessarily identical or constant over time.

There is only one output of the system: **PTT**. The 11 input physiological variables are:

1. **Bival rate**: the Bivalirudin injection rate which is the unique controllable input in our system.
2. **GFR** (mL/min): the Glomerular filtration rate, reflecting the ability of the kidneys to eliminate bivalirudin. Decreased GFR increases the serum level of bivalirudin and the PTT in an approximately linear fashion.
3. **PTT** (s): last measured partial thromboplastin time.
4. **INR** (Unit-less): the last measured international normalized ratio which is a coagulation time that is distinct, but associated with the PTT. This increases as the serum level of bivalirudin increases.
5. **SGOT** (Units/L): the Serum Glutamic Oxaloacetic Transaminase.
6. **SGPT** (Units/L): the Serum Glutamic Pyruvic Transaminase. Increasing SGOT and SGPT reflects liver dysfunction and decreased production of clotting factors, thus, increasing PTT.
7. **TBILI** (mg/dL): total bilirubin, a “waste product” normally eliminated by the liver. In liver dysfunction, this is positively associated with a rising PTT.
8. **ALB** (g/L): Albumin. which is reduced under liver failure and is therefore associated with a rising PTT.
9. **PLT** (K/mcL): Platelet count. Platelets help form blood clots with clotting factors from the liver. They are utilized when a clot is formed. A decreasing platelet count can indicate ongoing clotting with consumption of clotting factors, thus, elevating the PTT and INR.
10. **HCT** (%): Hematocrit. HCT is a measure of the amount of red blood cells in the blood. When patients loose blood during operations and other non-operative bleeding, then fluids such as normal saline are provided to make up for the blood volume lost. This, however, lowers the HCT. At the same time, the added volume dilutes the clotting factors in the blood and causes PTT and INR to increase.
11. **FIB** (mg/dL): Fibrinogen. This protein helps produce clots and its decreased concentration may indicate that clotting is occurring. It follows that clotting factors are being depleted which causes elevated PTT and INR.

B. The model

According to the interpretation of relationships among the PTT value and the other 11 predictors introduced before, we propose the dynamic system model of Fig. 1 to describe the process of PTT elimination. Due to a lack of established quantitative models to relate most of the above laboratory variables to the PTT, a simple linear model was assumed. Since many of these variables change slowly (over the course of days) and are measured infrequently (typically once per day), they were modeled without a dynamic component. The dynamic system model has been implemented in Matlab/Simulink. It seeks to represent how bivalirudin acts in a single generic patient; thus, and for ease of notation, we will suppress the patient identifier in our generic model description. In this dynamic system, there are 11 inputs which are denoted by $u_i(t)$, $i = 1, \ldots, 11$ and correspond to the physiological variables we have defined. The input $u_1(t)$, in particular, denotes the bivalirudin infusion rate, and the remaining inputs correspond to the physiological variables 2–11 detailed earlier. These inputs capture the patient's indicators of renal and liver function. There is only one output – the PTT value – which is denoted by $y(t)$. There is also a single state variable denoted by $x(t)$. The model has 14 unknown parameters: 13 of which correspond to the various gains and are denoted by β_i, $i = 1, \ldots, 13$. The initial condition of the system is the 14th unknown parameter and is denoted by $x(0)$. We will refer to $\mathbf{z} = (\beta_1, \ldots, \beta_{13}, x(0))$ as the parameter vector.

Let us write $\mathbf{u}(t) = (u_1(t), \ldots, u_{11}(t))$. The system dynamics can be expressed as follows:

$$\dot{x}(t)=\mathbf{A}x(t)+\mathbf{B}\mathbf{u}(t),\ y(t)=\mathbf{C}x(t)+\mathbf{D}\mathbf{u}(t), \quad (1)$$

where $\mathbf{A} = -\beta_3$, $\mathbf{B} = [\beta_1\ 0 \cdots 0]$, $\mathbf{C} = \beta_2$, and $\mathbf{D} = [0\ \beta_4 \cdots \beta_{13}]$. Clearly, this is a *Linear Time Invariant (LTI)* dynamic system. The challenge is that we only have sampled input, $\mathbf{u}(t)$, and observation values, $y(t)$, at certain times t for each patient. It is therefore needed to translate the continuous-time system dynamics to discrete-time dynamics.

Using a standard conversion from continuous to discrete time dynamics in LTI systems (see e.g., [5]) we can write

$$x(t+\tau)=e^{\mathbf{A}\tau}x(t)+\int_t^{t+\tau} e^{\mathbf{A}(t+\tau-s)}\mathbf{B}\mathbf{u}(s)ds, \quad (2)$$

where in our case $e^{\boldsymbol{\tau}\mathbf{A}} = e^{-\beta_3\boldsymbol{\tau}}$. Assuming $\mathbf{u}(s) = \mathbf{u}(t)$ for $s \in [t, t + \boldsymbol{\tau}]$ and after some algebra we arrive at the following discrete-time dynamics:

$$x(t+\tau)=e^{-\beta_3\tau}x(t)+\frac{\beta_1}{\beta_3}(1-e^{-\beta_3\tau})u_1(t),\ y(t)=\beta_2 x(t)+\sum_{i=4}^{13}\beta_i u_{i-2}(t). \quad (3)$$

These equations characterize a discrete-time LTI system for which we have a history of sampled input and output values. Next we describe how this training set can be used to identify the unknown parameters, namely, the initial condition $x(0)$ and the parameters β_i, $i = 1, \ldots, 13$.

C. Parameter Identification

We randomly split our data set of 233 post-cardiac surgical ICU patients into a training set corresponding to 2/3 of the total (155 patients) and a test set corresponding to 1/3 of the total (78 patients). We will use the former to identify the unknown system parameters and the latter to evaluate the performance of the resulting model.

Let us use a subscript j to denote the model primitives, i.e., the state $x_j(t)$, output $y_j(t)$, and inputs $\mathbf{u}_j(t)$ for each patient $j = 1, \ldots, N$, where N denotes the number of patients in the training set. To distinguish between measurements of $y_j(t)$ and predictions based on the system dynamics (cf. (3)) we use $y_j(t)$ for the former and $\hat{y}_j(t)$ for the latter. Suppose for each patient j we have T_j measurements at times $t_j^1, \ldots, t_j^{T_j}$, where we adopt the convention $t_j^0=0$ for all j. Using the discrete-time system dynamics from (3) we formulate the following nonlinear optimization problem in order to identify the unknown system parameters:

$$\begin{aligned} \min \quad & \textstyle\sum_{j=1}^{N}\sum_{t=t_j^1}^{t_j^{T_j}}(\hat{y}_j(t)-y_j(t))^2 \\ \text{s.t.} \quad & x_j(t_j^n)=e^{-\beta_3(t_j^n-t_j^{n-1})}x_j(t_j^{n-1})+\tfrac{\beta_1}{\beta_3}(1-e^{-\beta_3(t_j^n-t_j^{n-1})})u_{j,1}(t_j^{n-1}), \forall j=1,\ldots,N; n=1,\ldots,T_j, \\ & \hat{y}_j(t_j^n)=\beta_2 x_j(t_j^n)+\textstyle\sum_{i=4}^{13}\beta_i u_{j,(i-2)}(t_j^n) \forall j=1,\ldots,N; n=1,\ldots,T_j, \end{aligned} \tag{4}$$

where the decision variables are $x(0)$(= $x(t_j^0)$ for all j) and the parameters β_i, $i = 1, \ldots, 13$. One can easily substitute the expressions from the constraints into the objective function and obtain a nonlinear unconstrained optimization problem. Using counterexamples, it can be shown that the objective function obtained in this manner is not convex in the decision variables.

Although a lot of methods exist for unconstrained optimization, we used the *Broyden-Fletcher-Goldfarb-Shanno (BFGS) method* [1], which is considered the most effective general purpose quasi-Newton method. Quasi-Newton methods are gradient methods of the form

$$\mathbf{z}^{k+1}=\mathbf{z}^k+\alpha^k\mathbf{d}^k, \mathbf{d}^k=-\mathbf{D}^k\nabla f(\mathbf{z}^k),$$

where $f(\cdot)$ denotes the objective function, $\mathbf{z}^k$ the decision variables at the kth iteration of the method, α^k is the stepsize at the kth iteration, and $\mathbf{D}^k$ is a positive definite scaling matrix that scales the gradient at the kth iteration. Rather than determining $\mathbf{D}^k$ by computing a Hessian and inverting it, which is computationally expensive, quasi-Newton methods recursively estimate the inverse of the Hessian by using successive iterates of $\mathbf{z}^k$ and $\nabla f(\mathbf{z}^k)$.

For performance evaluation, we use two performance metrics. The first is the *Root Mean Square Error (RMSE)*, which for patient i is defined as

$$\mathrm{RMSE}_i=\sqrt{\frac{1}{T_i}\sum_{t=t_i^1}^{t_i^{T_i}}(\hat{y}_i(t)-y_i(t))^2}, \tag{5}$$

where $t_i^1, \ldots, t_i^{T_i}$ are the time instants at which we make a PTT prediction for patient *i*. We define RMSE for the whole population of patients as the average per patient RMSE, i.e., $\mathrm{RMSE} = \frac{1}{N}\sum_{i=1}^{N} \mathrm{RMSE}_i$, where *N* is the number of patients in the test set. We also define σ_{RMSE} to be the standard deviation of the RMSE_i values, which captures the variability of RMSE_i from RMSE.

To capture a notion of "relative" error we also compute the *Normalized Root Mean Square Error (NRMSE)* defined for each patient *i* as

$$\mathrm{NRMSE}_i = \sqrt{\frac{1}{T_i}\sum_{t=t_i^1}^{t_i^{T_i}} [(\hat{y}_i(t) - y_i(t))/y_i(t)]^2}. \quad (6)$$

As with the RMSE, we define the population-wide NRMSE as the average of NRMSE_i over the patients and σ_{NRMSE} as the standard deviation of the NRMSE_i values.

We solved (4) on the training set using BFGS and obtained the solution shown in Table I. To avoid getting stuck at shallow local minima, which is possible in the absence of convexity, we used a multi-start approach, namely, we started BFGS from multiple randomly selected initial points and selected the best local minimum we obtained. Using the optimal parameters from Table I, we evaluated the performance of the predictor on the test set and obtained the results shown in Table II. We note that our model uses just a single state and, as it can be inferred from (3), the prediction at time *t* depends on the inputs $\mathbf{u}(t)$ at *t*, and the state-input pair, $x(t - \boldsymbol{\tau})$ and $\mathbf{u}(t - \boldsymbol{\tau})$ at the previous time instant $t - \boldsymbol{\tau}$.

To further illustrate how well the predictor matches the measured values we plot in Fig. 2 predicted and actual PTT values over time for a particular randomly selected patient.

The model we devised in this section is a generic population-wide model in the sense that its parameters have been trained from a collection of patients. As we will see in the next section, having an explicit model allows us to adapt model parameters to better fit each individual patient.

III. An adaptive model: Extended Kalman filter

In this section we focus on an arbitrary individual patient and seek a method to adapt the parameters of the model we proposed in Section II in order to better fit this particular patient. To that end, we view the model parameters as the "state" of a system and the output $y(t)$ as a nonlinear function of that state. We devise a recursive method to estimate the state. Due to the nonlinearity of $y(t)$ we use the *Extended Kalman Filter (EKF)* (see e.g., [8]).

Let us denote the state of the system by $\mathbf{z} = (\beta_1, \ldots, \beta_{13}, x(0))$, which are exactly the model parameters we want to estimate. We assume we have measurements of the inputs $\mathbf{u}(t)$ and the PTT values $y(t)$ over many time instants. We will index these time instants by *k*, with $k = 0$ corresponding to $t = 0$ and $k = 1, 2, \ldots, T$ corresponding to the time instants $t^1, \ldots, t^T$ at which we have measurements. (Notice we use the same notation as in Section II but suppress the index *j* used there to identify a patient.) We view the state $\mathbf{z}$ as been invariant

over time and not affected by noise, while the output y depends on $\mathbf{z}$ but is subject to some noise due to both measurement noise and model error. We can therefore write the (discrete) system dynamics as:

$$\mathbf{z}_k = \mathbf{z}_{k-1}, \; y_k = h(\mathbf{z}_k) + \nu_k. \quad (7)$$

In the above, $h(\cdot)$ is a known nonlinear function that expresses y_k as function of the parameter vector $\mathbf{z}_k$ and $\mathbf{u}_k$, $\mathbf{u}_{k-1}$, …, $\mathbf{u}_0$, x_0 as specified by the dynamics in (3). The random variable ν_k represents the noise and we assume it is i.i.d. over time, zero mean Gaussian, with variance σ^2, that is $\nu_k \sim N(0, \sigma^2)$ for all k.

Let $\mathbf{A} = \mathbf{I}$, and $\mathbf{C} = \nabla h'(\mathbf{z}_k)$. The EKF algorithm is given in Fig. 4, where "hat" denotes the estimate, $\mathbf{P}$ the error covariance, and $\mathbf{K}$ the Kalman gain.

To demonstrate the effect of this algorithm, we randomly selected a patient who has adequate sample data and applied the EKF algorithm of Fig. 4 (using $\sigma^2 = 0.006$). The results are shown in Fig. 3. After some initial steps, the algorithm "learns" better values for the model parameters than the ones in the population-wide model and produces better predictions for this particular patient. The model parameter values for the same patient during the course of the EKF algorithm are shown in Fig. 5. It can be seen that they do "adapt" over time from the initial population-wide values to values that are more appropriate for this patient.

To test the performance of the algorithm on a larger set of patients, we selected patients with enough samples and applied the EKF (using again $\sigma^2 = 0.006$) with the optimal population wide parameter values as our initial point. By doing so, the time the EKF needs for the model parameters to converge can be reduced significantly. If, instead, we choose an arbitrary initial point, the EKF takes at least 25 steps for the parameter values to stabilize. The rather large prediction error during these initial steps can compromise patient safety and is therefore unacceptable. Results for a subset of 6 patients are shown in Table III. The RMSE and NRMSE reported are computed on the time series that excludes a number of initial samples, thus, evaluating performance after the EKF has the chance to adapt to the individual patient. It can be seen that for several patients, the performance becomes better than the average performance obtained from the population-wide model (cf. Table II).

Table IV reports average results from the EKF algorithm applied to a collection of patients that have adequate sample points. RMSE and NRMSE are computed on a per-patient basis and then averaged over these patients. It can be seen that average performance improves compared to the population-wide model and the variance drops. As we have discussed earlier, performance for individual patients can improve much more significantly. Further, and because the model adapts to each individual patient, error variance across patients drops significantly.

IV. Conclusions

We have developed an approach to predict the effect of bivalirudin in cardiac surgical patients. Our approach is *model-based* and constructs a specific model that captures how

bivalirudin affects PTT values. Model parameter identification is done by solving a nonlinear optimization problem over a training set.

Our approach enables the development of an adaptive extended Kalman filtering algorithm that can adapt model parameters to individual patients. This improves the average performance compared to the population-wide model and drastically reduces the per-patient variance. More specifically, the standard deviation of the per-patient NRMSE is reduced by more than 40%, This shows that patient-specific models have significant advantages over population-wide models.

The mathematical models and prediction approaches described in this study may provide a better reference to guide the optimal therapy in cardiac patients in need of bivalirudin. In addition, such mathematical ideas and methods may be useful to test medication dosing strategies and may provide a mathematical mechanism for development and testing of nomograms.

REFERENCES

1. Bertsekas, DP. Nonlinear Programming. 2nd edition. Belmont, MA: Athena Scientific; 1999.
2. Bittl JA, Chaitman BR, Feit F, Kimball W, Topol EJ. Bivalirudin versus heparin during coronary angioplasty for unstable or postinfarction angina: final report reanalysis of the bivalirudin angioplasty study. American heart journal. 2001; 142(6):952–959. [PubMed: 11717596]
3. Edrich T, Frendl G, Paschalidis ICh. Tachyphylaxis in post-cardiac surgical patients receiving bivalirudin – a retrospective dynamic study using a PKPD model. Critical Care Medicine. 2011 Dec.39(12):198.
4. Edrich, T.; Frendl, G.; Rawn, J.; Paschalidis, ICh. Modeling the effects of bivalirudin in cardiac surgical patients. Proceedings of the 33rd Annual International IEEE Conference of the Engineering in Medicine and Biology Society (EMBS); August 30–Sept. 3 2011; Boston, Massachusetts. p. 120-123.
5. Friedland, B. Control system design: an introduction to state-space methods. Dover Publications; 2005.
6. Lincoff AM, Bittl JA, Harrington RA, Feit F, Kleiman NS, Jackman JD, Sarembock IJ, Cohen DJ, Spriggs D, Ebrahimi R, et al. Bivalirudin and provisional glycoprotein IIb/IIIa blockade compared with heparin and planned glycoprotein IIb/IIIa blockade during percutaneous coronary intervention. JAMA: the journal of the American Medical Association. 2003; 289(7):853–863. [PubMed: 12588269]
7. Stone GW, McLaurin BT, Cox DA, Bertrand ME, Lincoff AM, Moses JW, White HD, Pocock SJ, Ware JH, Feit F, et al. Bivalirudin for patients with acute coronary syndromes. New England Journal of Medicine. 2006; 355(21):2203–2216. [PubMed: 17124018]
8. Welch, G.; Bishop, G. Technical Report TR 95-041. Chapel Hill: Dept. of Computer Science, Univ. of North Carolina; 2006. An introduction to the Kalman filter.

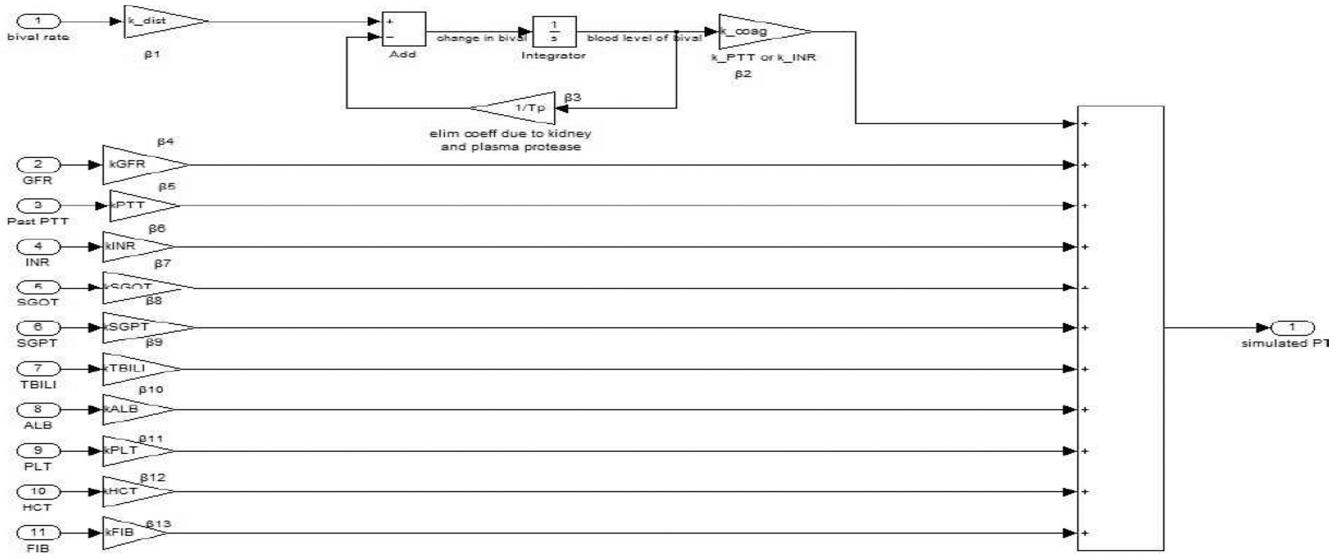

Fig. 1.

The single-state linear model includes a gain, $1/Tp(\beta_3)$, representing the elimination time constant of bivalirudin from the body. The constant k_{PTT} (β_2) provides for the translation from serum concentration to the site-effect (PTT). We build this model based on the interpretation of relationships between PTT and these predictors.

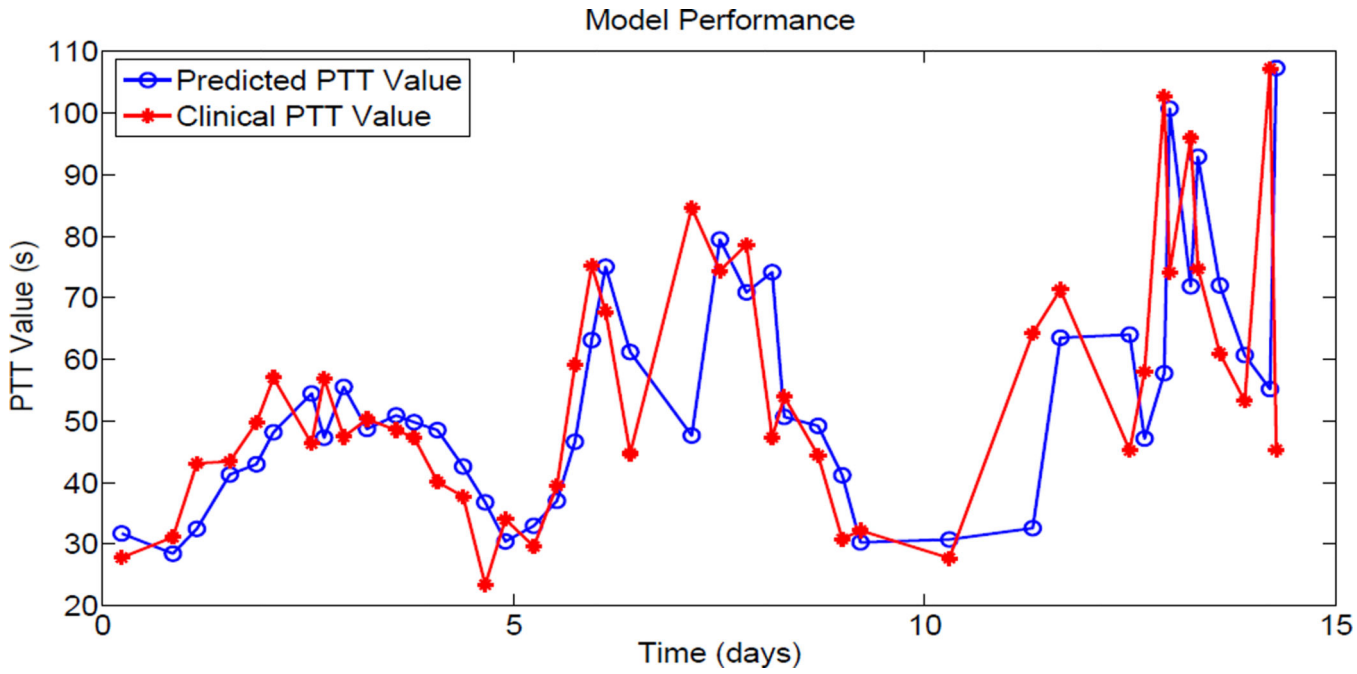

Fig. 2.

Illustrating the performance of the dynamic system model of Sec. II for a particular patient. The blue + represent predicted PTT values from our model and the red * represent actual measured values.

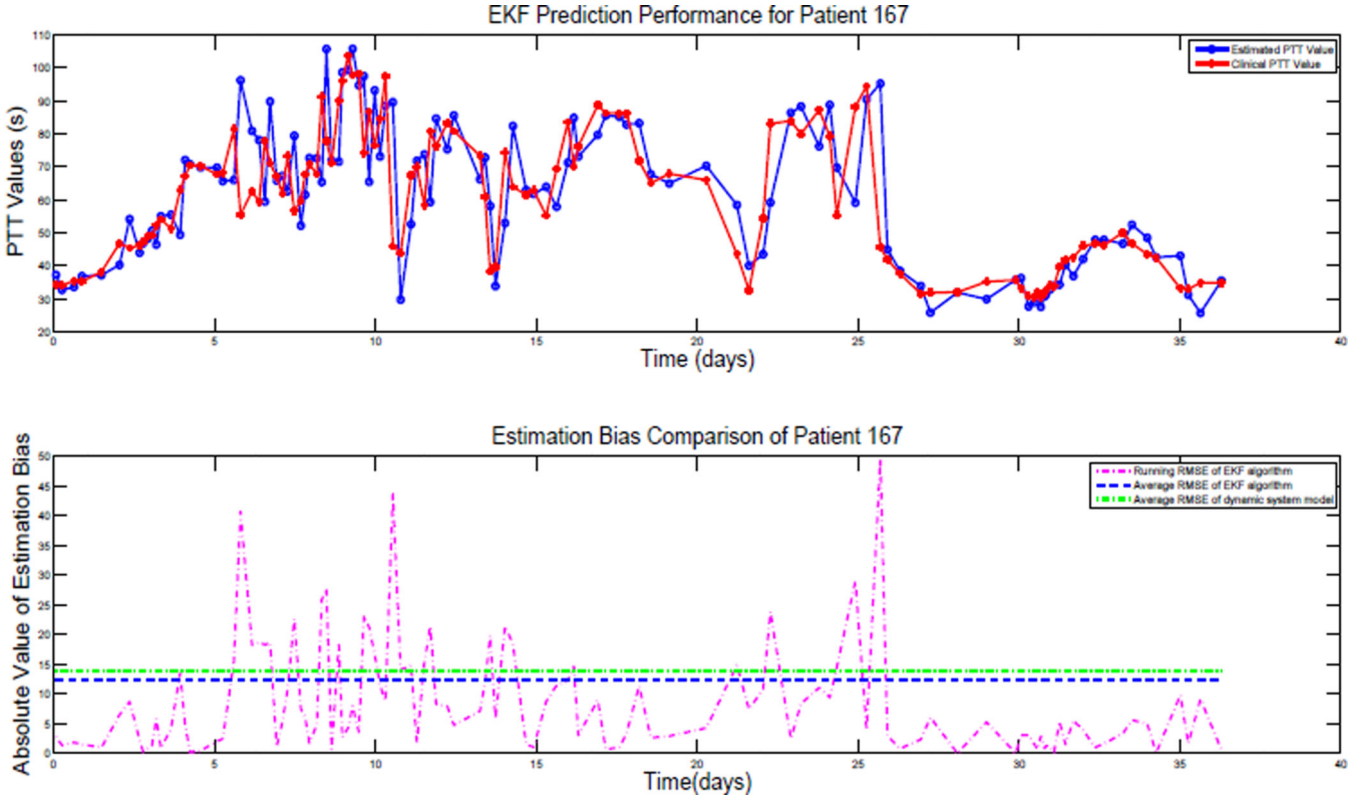

Fig. 3.

Illustrating the performance of the EKF algorithm for a particular patient. The blue “o” represent predicted PTT values from our model and the red “*” represent actual measured values. The top figure plots estimated and measured PTT and the bottom figure plots the running RMSE at each step. Additionally, the blue-dot line marks the (time) average RMSE of the EKF for this patient while the green-dot line marks the (time) average RMSE of the population-wide dynamic system model applied to this patient.

1) Initialization:
   a) Set $\hat{\mathbf{z}}_{0|0} = (\beta_1, \ldots, \beta_{13}, x(0))$ using the values obtained by solving the population-wide problem (4), and
   b) set $\mathbf{P}_{0|0} = \mathbf{I}$.
2) Predict:
   a) $\hat{\mathbf{z}}_{k+1|k} = \hat{\mathbf{z}}_{k|k}$;
   b) $\mathbf{P}_{k+1|k} = \mathbf{A}\mathbf{P}_{k|k}\mathbf{A}'$.
3) Update:
   a) $\mathbf{K}_{k+1} = \mathbf{P}_{k+1|k}\mathbf{C}'(\mathbf{C}\mathbf{P}_{k+1|k}\mathbf{C}' + \sigma^2)^{-1}$;
   b) $\hat{\mathbf{z}}_{k+1|k+1} = \hat{\mathbf{z}}_{k+1|k} + \mathbf{K}_{k+1}(y_{k+1} - h(\hat{\mathbf{z}}_{k+1|k}))$;
   c) $\mathbf{P}_{k+1|k+1} = (\mathbf{I} - \mathbf{K}_{k+1}\mathbf{C})\mathbf{P}_{k+1|k}$.

Fig. 4.
The EKF algorithm for recursively estimating model parameters for an individual patient.

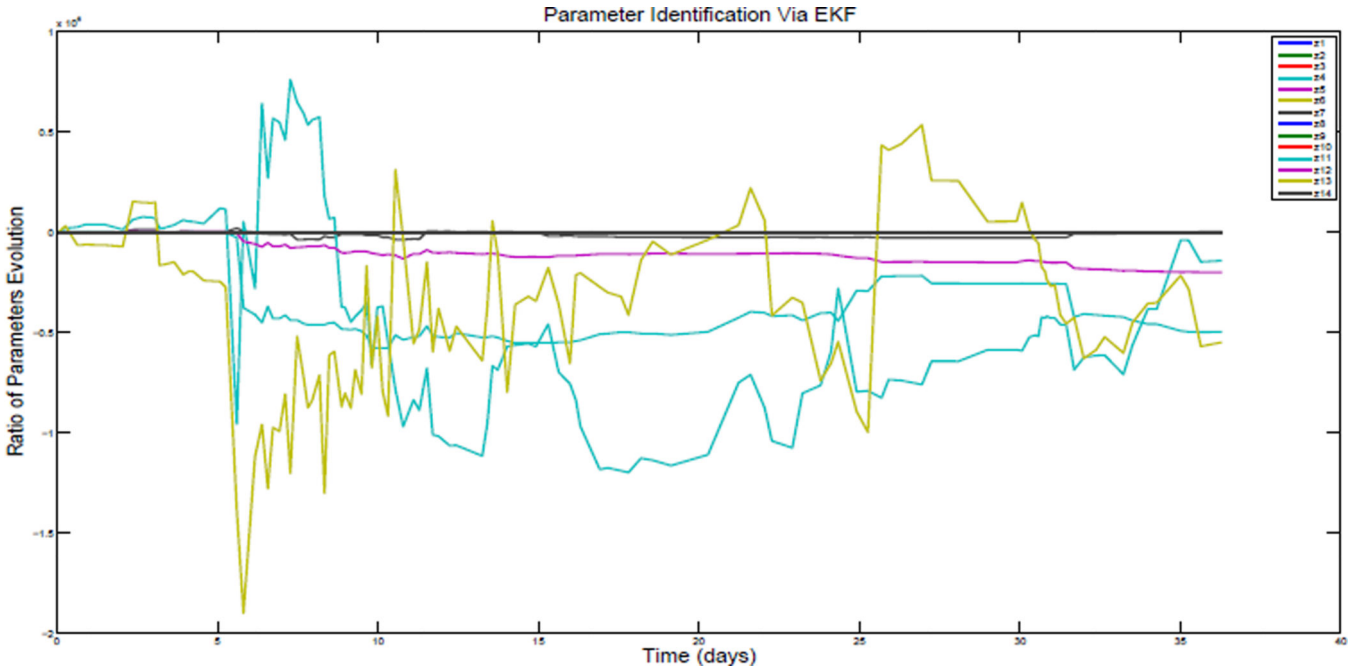

Fig. 5.

Illustrating the evolution of model parameter values $\mathbf{z} = (\beta_1, \ldots, \beta_{13}, x(0))$ during the course of EKF algorithm.

TABLE I

Optimal Parameters Values

index	name	value
1	k_dist (β_1)	22.2718
2	k_coag (β_2)	18.6109
3	1/T (β_3)	6.2084
4	kGFR (β_4)	−0.0273
5	kINR (β_5)	0.5296
6	kPTT (β_6)	−0.8013
7	kSGOT (β_7)	0.0004
8	kSGPT (β_8)	0.0018
9	kTBILI (β_9)	0.1266
10	kALB (β_{10})	2.0183
11	kPLT (β_{11})	−0.0011
12	kHCT (β_{12})	0.5782
13	kFIB (β_{13})	0.0089
14	$x(0)$ (β_{14})	−1.1785

TABLE II

Performance of the dynamic system model

RMSE	12.97
σ_{RMSE}	5.2
NRMSE	24.12%
σ_{NRMSE}	9.04%

TABLE III

EKF Performance for a collection of patients

Patient ID	# of Samples	RMSE	NRMSE
94	108	14.23	26.00%
167	119	12.19	25.22%
176	236	8.57	15.36%
189	114	13.18	23.21%
198	114	9.69	22.01%
217	160	11.80	22.10%

TABLE IV

Performance of The EKF algorithm

RMSE	11.61
σ_{RMSE}	2.13
NRMSE	22.53%
σ_{NRMSE}	3.64%